No Free Lunch for Avoiding Clustering Vulnerabilities in Distributed Systems

Pheerawich Chitnelawong,[1] **Andrei A. Klishin,**[2,3] **Norman MacKay,**[1] **David J. Singer,**[4] **Greg van Anders**[1]

[1]Department of Physics, Engineering Physics, and Astronomy, Queen's University, Kingston ON, K7L 3N6, Canada

[2]Department of Mechanical Engineering, University of Washington Seattle, WA 98195, USA

[3]AI Institute in Dynamic Systems, University of Washington, Seattle, WA 98195, USA

[4]Department of Naval Architecture and Marine Engineering University of Michigan, Ann Arbor, MI 48109, USA

E-mail: `gva@queensu.ca` (Greg van Anders)

Abstract. Emergent design failures are ubiquitous in complex systems, and often arise when system elements cluster. Approaches to systematically reduce clustering could improve a design's resilience, but reducing clustering is difficult if it is driven by collective interactions among design elements. Here, we use techniques from statistical physics to identify mechanisms by which spatial clusters of design elements emerge in complex systems modelled by heterogeneous networks. We find that, in addition to naive, attraction-driven clustering, heterogeneous networks can exhibit emergent, repulsion-driven clustering. We draw quantitative connections between our results on a model system in naval engineering to entropy-driven phenomena in nanoscale self-assembly, and give a general argument that the clustering phenomena we observe should arise in many distributed systems. We identify circumstances under which generic design problems will exhibit trade-offs between clustering and uncertainty in design objectives, and we present a framework to identify and quantify trade-offs to manage clustering vulnerabilities.

1. Introduction

A key challenge in the design of complex, large-scale systems is managing emergent vulnerabilities [1, 2, 3, 4, 5], especially those driven by clustering. Examples of cluster-driven vulnerabilities include failures in communication networks such as the Internet [6, 7, 8], hot spot leakage in microprocessors [9, 10], congestion in airline networks [11, 12], and high outfit density in naval engineering [13, 14]. Though clustering vulnerabilities are inherently local, they typically degrade global, network-wide performance. For example, mitigating isolated hot spots in microprocessors frequently involves throttling the performance of the entire device [15, 16, 17]; or damage to a single shipboard system can cause co-located systems to fail, inducing failures that cascade through the ship [18, 19, 20, 21]. Guidance for mitigating clustering instabilities is therefore critical across many engineering domains.

Clustering vulnerabilities are ubiquitous in complex system design [22, 23, 3, 2] because, in systems comprised of a large number of functional units, units are often arranged to minimize physical connection distances. Distance-minimization drivers can be economic, e.g., minimizing material cost [24, 25], or physical, e.g., minimizing energy loss or latency [26, 27, 28], or a combination of economic and physical [29]. Regardless of the driver, connection-distance minimizing arrangements of design elements induce spatial grouping, and that grouping produces clustering vulnerabilities [30, 31]. Approaches to reduce clustering vulnerabilities in general therefore need to disrupt the drive for short connection distances.

Since clustering vulnerabilities arise generically in the optimization of systems with complex inter-dependencies, there are two obvious strategies to mitigate such vulnerabilities. One obvious mitigation strategy is to make ad hoc modifications to the optimization criteria to counteract the clustering that produces the vulnerability. However, vulnerabilities are most difficult to manage in the system that they are most likely to arise in, e.g., complex systems described by large, he of connected elements [1]. Because emergent vulnerabilities occur unpredictably, actions to mitigate one vulnerability may induce the emergence of others, which could be more numerous or severe than the original. If modifying optimization criteria ad hoc to mitigate one vulnerability can drive the emergence of others, a second alternative strategy could be to look beyond strictly optimal solutions in a systematic way. In situations where economic considerations factor among optimization criteria considering non-optimal solutions is, in a colloquial sense, buying a way out of the problem. However, employing expensive, sub-optimal solutions could be a worthwhile sacrifice if the vulnerabilities induced by clustering are severe, and if sub-optimal solutions reliably eliminate clustering.

Here, we show that a complex interplay between how design elements are physically placed and how their functional connections are placed defeats simple strategies to mitigate cluster-driven vulnerabilities. We argue that in generic situations in which there are multiple possible choices of connection routes for each given placement of functional elements in a fixed spatial region, routing multiplicity is the dominant driver of element

placement when connection-distance minimization is relaxed. In relaxed distance-minimization settings, we find that routing multiplicity and connection heterogeneity combine to drive new, emergent forms of clustering. This emergent clustering defeats naive "buy out" approaches to mitigate clustering vulnerabilities. By connecting routing and placement multiplicity to analogous concepts of configurational and conformational entropy in physical systems, we show that it is possible to avoid clustering by managing a balance between placement and routing multiplicity, but that this can only be achieved at the expense of high uncertainty in the original optimization objectives. We give a concrete illustration of these effects via a detailed analysis of a problem in Naval Engineering. Our results show there is no simple, one-size-fits-all approach to managing clustering vulnerabilities. However, we show that clustering vulnerabilities can be managed in a context-dependent, case-by-case manner using a consistent framework.

2. Results

2.1. Clustering in a Model System

To motivate a general argument on clustering vulnerabilities, it is instructive to first understand how they arise in a specific example. We use a system from naval architecture that describes arranging the power system of a naval vessel inside a ship hull. [13] The model describes the placement of elements of the power system and their interconnections, with a cost associated with connection length (see Methods section 4). This model has two features that are exemplary of other contexts: (i) optimizing arrangements for short connection distances drives system elements to cluster in space [32]; (ii) because the network is comprised of elements that are power sources and power sinks, the connectivity of the network is heterogeneous; i.e., it has both high- and low-connectivity elements.

We study this model by generating candidate arrangements controlled by a parameter T (see Methods section 4) that serves as a tolerance for generating non-minimal routing distances, and is mathematically equivalent to temperature (see Methods section 4). $T = 0$ indicates no tolerance for non-minimal routing distance and $T \to \infty$ indicates unlimited tolerance for non-minimal routing distance. Results below parametrize T relative to a crossover value T_c that we determine by comparing classes of model results (see Methods section 4).

Figure 1 reports clustering behaviours in our model system. We use two types of measure: global and local. The global measure, radius of gyration, reports average 'pair-wise' (two-point) correlation between all pairs, regardless of the position of the design element in the ship. The local measure reports an average one-point correlation over all design elements over different locations of the ship hull. We report both global measures of clustering (panel E) and local measures in the ship hull (panels C, D, F, G) at a range of tolerances for non-minimal route length.
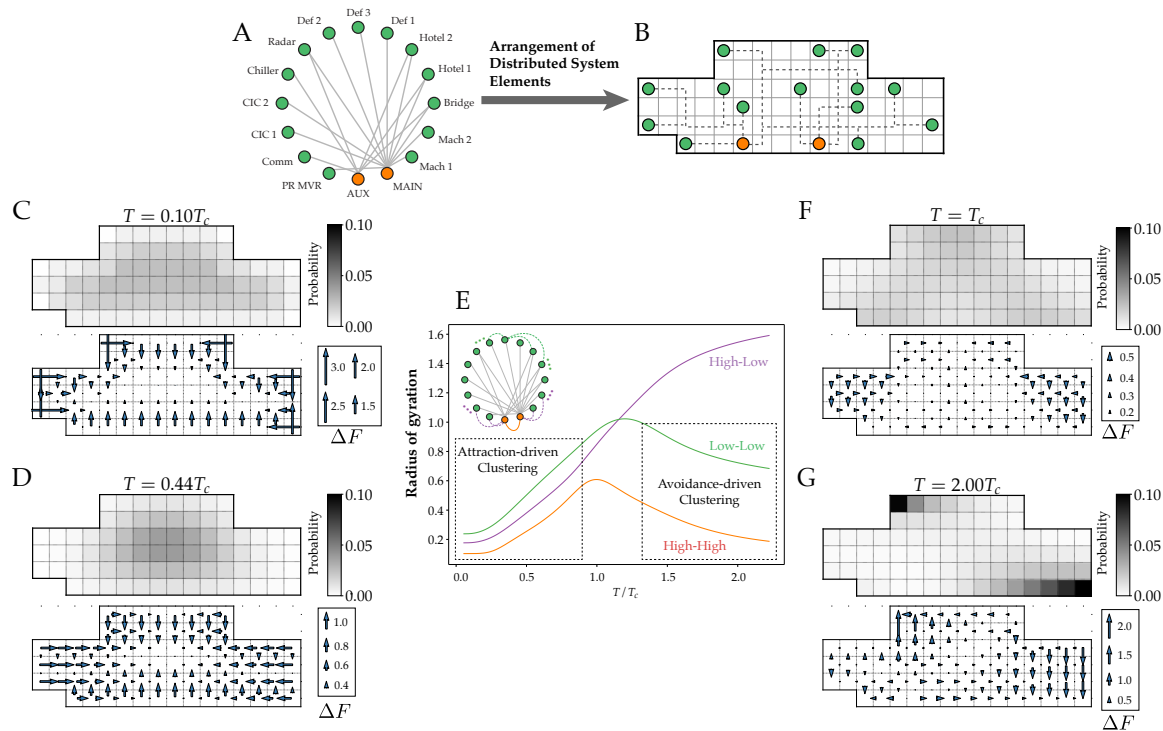
Figure 1.   Avoidance-driven clustering emerges in non-minimal distance routing.   Panel A illustrates design-element connectivity of a shipboard power systems.   Panel B illustrates a hypothetical arrangement.   Panel E plots radius of gyration (R_g) versus T that quantifies correlations between elements paired by their degree of connectivity, low-low, high-high, and high-low. Low R_g at low T, where designs are dominated by minimal routing distance are clustered by attraction. However, low R_g at high T for functionally disconnected, low-low and high-high connectivity pairs that coincides with high R_g for functionally connected high-low pairs indicates repulsion driven clustering. The inset network diagram shows example element pairs that R_g is averaged over. Panels C, D, F, and G show element localization in the ship hull. Low T clustering (C and D) is expected since the objective prioritizes routing cost, and the distribution is a single dense region, that is central, and excludes the boundary, all consistent with attraction-driven clustering. High T clustering (G), however, is multi-modal and peripheral. Moderate T (F) corresponds to local peaks in R_g (panel E) and is distributed throughout the hull which indicates de-clustering.

2.1.1. Global Measures Show Emergent Clustering of Non-Connected Elements. We note that the underlying form of the power system as a set of objects "tethered" to one another by functional connections is reminiscent of polymer systems. So, we borrow from polymer physics and measure global clustering via the radius of gyration, R_g,[33] a root-mean-squared distance between a set of objects (see Methods section 4). As expected, at low T we find that power system elements are tightly clustered, regardless of their degree of network connectivity, as indicated by low gyration radii.

More surprisingly, however, we find that clustering re-emerges when T is high. Figure 1E shows that although R_g approaches the size of the space for directly connected power system elements (all of which are high-low connectivity pairs), R_g is small for

unconnected power system elements (low-low and high-high connectivity pairs). This form of clustering is striking for two reasons: because clustering involves subsets of the elements, and because the elements that cluster together are ones that don't have direct functional connections.

2.1.2. Local Measures Show Emergent Clusters are Peripheral. To understand the origin of emergent clustering, we analyzed the local distribution of power system elements throughout the ship hull. We first establish a baseline for comparison by computing element distributions at low T, where we expect conventional attraction-driven clustering.

Figure 1C shows the distribution of power system elements in arrangements driven by attraction-driven clustering. The global measure of clustering at low T in Figure 1E indicated that the system elements form a cluster with small R_g. The local distribution in Figure 1C shows that the global clustering coincides with arrangements with a near-uniform distribution throughout the ship hull. Note that the exception to uniformity is the depleted region near the boundary. This behaviour is analogous to the behaviour of polymer solutions confined, for example, within a tube with repulsive walls where the conformational entropy, i.e., internal rearrangements, of the polymer reduce the density of the solution near the walls [34]. As further confirmation, increased but still relatively low T (from $0.2T_c$ to $0.4T_c$) produces clusters with increased R_g, which lead to element distributions with a wider depleted boundary layer. These distributions share three features: a single dense region, central distribution, and boundary exclusion.

However, distributions at high T reverse all three features: high T distributions that they are multi-modal, not centred, and do not exclude the boundary. On the contrary, Figure 1G shows that high T ($T = 2T_c$) generates element distributions that exclude the central region; instead they localize on the boundary in two distinct regions. The existence of these two regions accords with the global R_g clustering measure: Figure 1E showed that functionally disconnected elements that had similar degrees of connectivity (low or high) formed clusters, whereas functionally connected elements had large R_g. The element distribution in Figure 1G suggests the differing clustering of functionally disconnected elements (low-low and high-high, which cluster) and functionally connected elements (high-low, which spread) arise because distinct regions of the element distributions correspond to elements with distinct degrees of connectivity.

2.1.3. Emergent, Peripheral Clusters Segregate by Degree of Connectivity. To determine whether cluster separation occurs because elements separate by degree of connectivity, we separately analyze the distribution of representative high-connectivity and low-connectivity power system elements in Figure 2. Computed distributions indicate that the two concentration areas in the connectivity-agnostic element distribution in Figure 1G can be associated with either high- or low- connectivity elements. Panels A and B in Figure 2 indicate that emergent clusters segregate elements
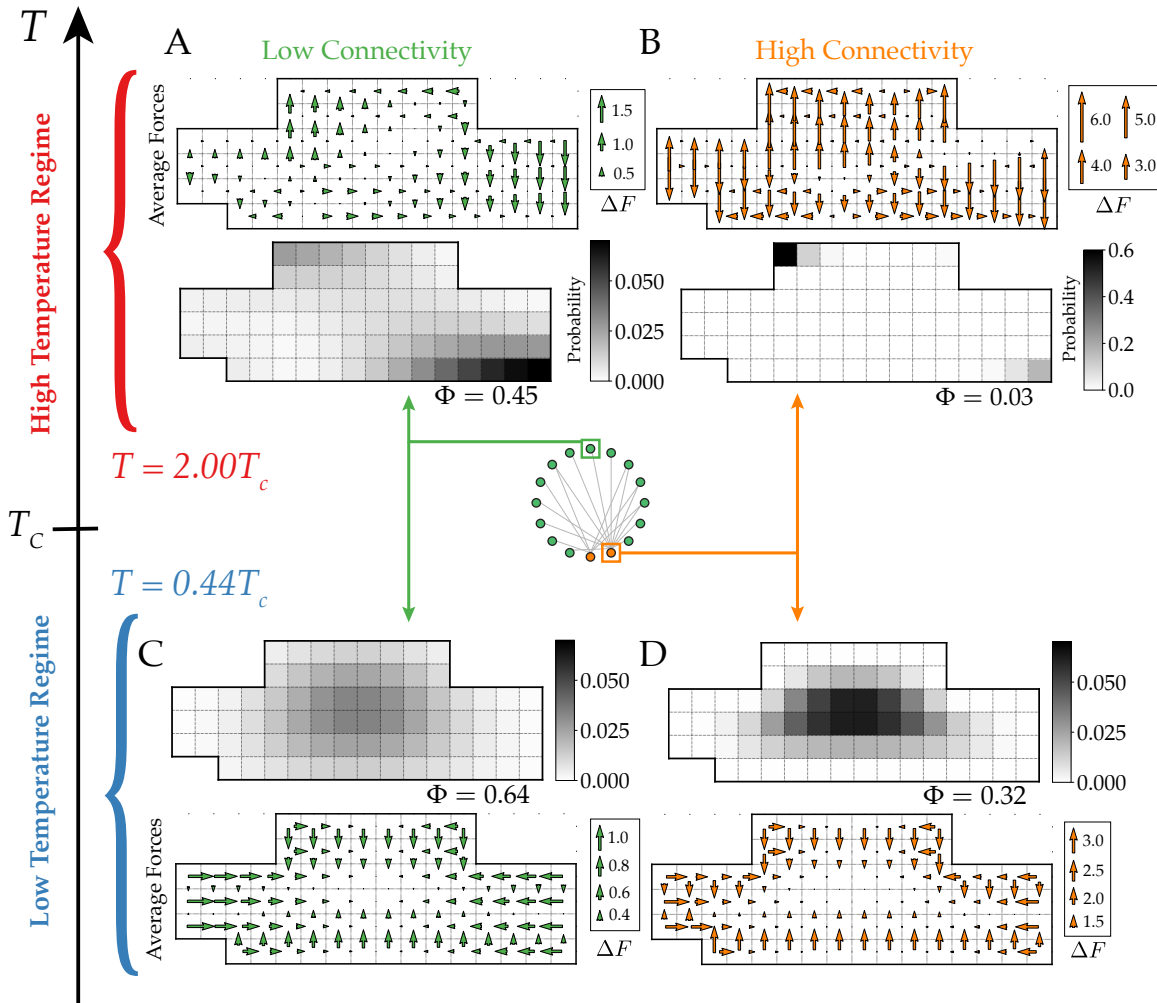
Figure 2. **Emergent clustering segregates design elements by degree of connectivity.** Panels A-D show probability distributions and effective forces for representative design elements that have low- (AC) or high- (BD) degrees of connectivity. Avoidance-driven clustering at high T in low-connectivity elements (A) and high-connectivity elements (B) display distinct behavior. Low connectivity elements adhere to the bottom right of the hull, and high-connectivity units localize near the top left. Effective forces (quiver plots) are larger for high-connectivity elements. Attraction-driven clustering at low T for low-connectivity (C) and high-connectivity (D) elements shows high-connectivity elements are more localized, which is consistent with the force measurements.

by their degree of connectivity.

For comparison, we computed distributions for the same elements at low T. Panels C and D in Figure 2 suggest that, while there is considerable overlap between distributions for high- and low-connectivity elements, high-connectivity distributions are more concentrated suggesting a "core-shell" form of spatial organization.

2.1.4. Routing Multiplicity Drives Emergent Clustering. The existence of clustering at low T is unsurprising, however the re-emergence of clustering when the preference for non-minimal routing is relaxed is unexpected. The fact that clusters form in separate, segregated, peripheral groupings violates the intuition power system elements should de-localize if the drive for minimal routing is relaxed.

To understand the origin of the unexpected emergent clustering, it is instructive to extend the analogy with conventional physical systems. The generating function for arrangements (see Methods section 4) can be decomposed into three sets of contributions: the length-dependent cost of routing connections between power system elements, the multiplicity of arrangements of power system elements with fixed route lengths, and the multiplicity of the routing paths for a fixed element arrangement and route lengths. These factors are analogous to line tension, configurational, and conformational entropy, respectively, in physical systems. The identification of these physical analogues gives a direction for further analysis.

The analogy between power system element arrangement multiplicity and configurational entropy suggests quantifying this contribution in terms of the spatial spread of the element distribution. In other contexts, existence area (see Methods section 4) is used to measure inhomogeneity in distributions that arises in localization.[35] Here, we use the same mathematical form to characterize the arrangement multiplicity of power system elements. Figure 3B shows this form of design freedom, which is a proxy for configurational entropy, as a function of T. Decreases in design freedom at low T and at high T are counter-intuitive because they indicate a loss of configurational entropy.

In thermodynamic systems, entropy conventionally increases monotonically with temperature, which is typically expressed in terms of a strictly positive heat capacity, C_V. Figure 3A,C show total system entropy and heat capacity as a function of T. Figure 3A shows that entropy is an increasing function of T as expected, and Figure 3C shows that the heat capacity is strictly positive. These results indicate that the reductions in design freedom with increasing T still coincide with increasing total entropy, but that this total entropy increase occurs because the conformational entropy associated with the existence of multiple routing paths between a fixed arrangement of elements overwhelms the configurational entropy associated with the multiplicity of element arrangement.

Taken together, five factors all suggest emergent clusters that are separate, segregated, and peripheral is driven by the generation of arrangements that are dominated by the multiplicity of routing paths for a fixed arrangement of power system elements: (i) the global clustering R_g (Figure 1E); local element distributions, both (ii) agnostic of connectivity (Figure 1G) and for representative (iii) low- (Figure 2A) and (iv) high-connectivity (Figure 2B) elements, and (v) contrasting design freedom and entropy measures.
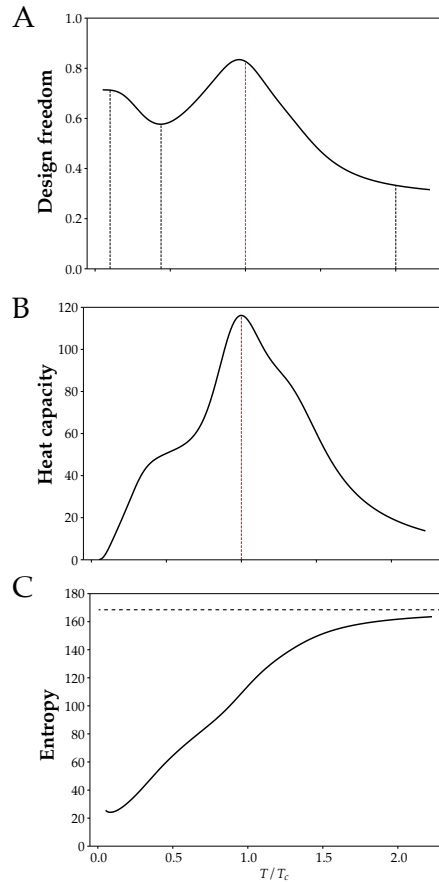
Figure 3. **Declustering coincides with high-variability in the design objective.** **Panel (A)** design freedom (a measure the freedom to place design elements, see Methods) vs T peaks at intermediate T, indicating declustering. **Panel (B)**, heat capacity vs T, indicates that declustering coincides with a peak in heat capacity. However, because heat capacity measures fluctuations in routing distance (see Methods), declustering coincides with maximal uncertainty in the primary design objective. **Panel (C)**, total system entropy vs T increases monotonically, as expected, indicating that decreasing design freedom at large T with cost tolerance occurs because routing multiplicity increases at the expense of unit placement multiplicity.

2.1.5. Declustering Coincides with Design Objective Variability. The above analysis showed that the unexpected re-emergence of clustering at high T was driven by entropic effects. However, this analysis also revealed a peak in the heat capacity in Figure 3C at intermediate T, and this raises the possibility of a different scenario to avoid clustering.

In systems of macroscopic numbers of atoms, sharp divergences in heat capacity signal a phase transition at a corresponding critical temperature. And, importantly, conventional thermodynamic systems at a critical point typically develop fractal behaviour, with spatial organization at many different scales [36]. Multi-scale organization is a possible "out" to the clustering problem, and could be achievable, not at high T where instead we observed re-emergent clustering, but at intermediate T.

The present system has a finite number of elements so the heat capacity cannot
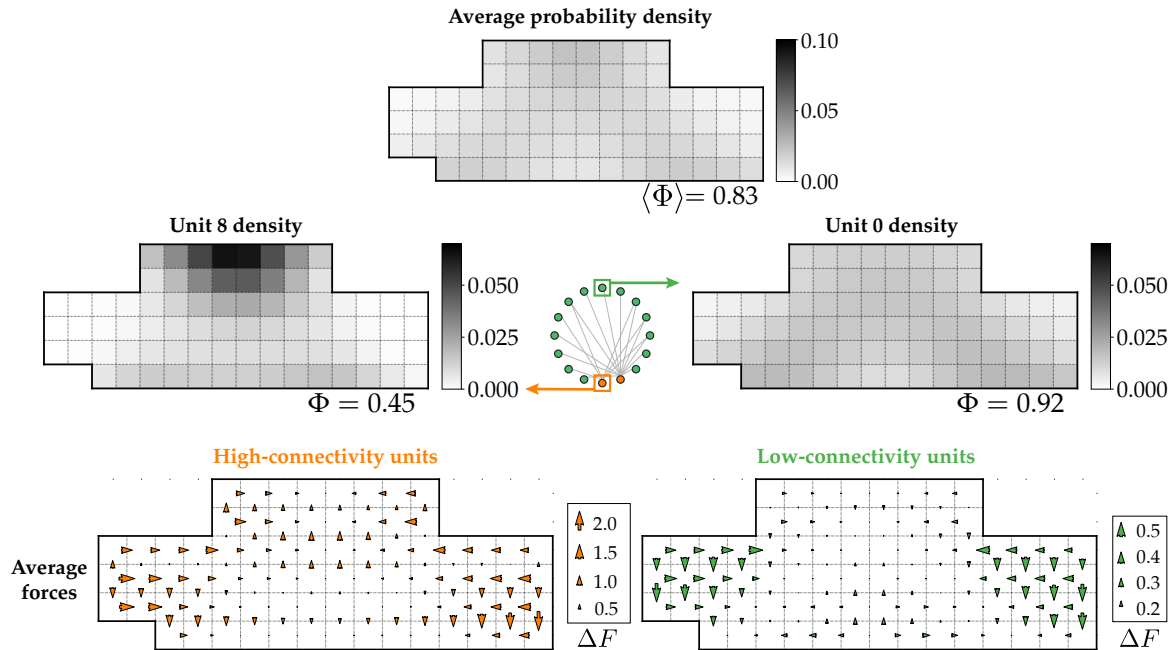
Figure 4. High variability configurations segregate by connectivity. High variability configurations at intermediate T ($T = T_c$) have distributions that differ by connectivity. High-connectivity units (left panels) localize more strongly than low-connectivity units (right panels).

exhibit a sharp divergence. However, despite the lack of a sharp divergence in heat capacity in the present system, quasi scale-invariant behaviour is possible. To investigate this we carried out global and local measures of clustering at T_c. Figure 1F shows that indeed power system elements distribute in both central and peripheral locations. This spread-out distribution approximately coincides with maximal R_g for non functionally-connected elements (Figure 1E), and a peak in design freedom (Figure 2B).

Furthermore, segregation by connectivity for high- and low- connectivity elements is also found at intermediate temperature as shown in Figure 4. However, the clustering behaviour is significantly mitigated with the average design freedom of 0.83 at $T = T_c$. This result emphasizes that connectivity-dependent localization is an inherent feature of a heterogeneous network that persists across all temperatures.

Together, the results indicate that in the vicinity of T_c there is a significant decrease in clustering. However, this decreased clustering comes at a price. Thermodynamic heat capacity serves as a measure of the size of energy fluctuations across a set of states. [37] Comparing the present system with thermodynamic systems, the role of energy is taken by the total routing cost, and so high heat capacity implies high routing cost uncertainty. This routing cost uncertainty, however, implies high variability in the main design objective. This means that in the present system, declustering coincides with high design objective variability.

2.2. Clustering by Repulsion-Driven Attraction in General

The clustering behaviour we observed in the naval architecture model arose from an interplay between the objective for minimal-length routes and two multiplicities: arranging power system elements and arranging the connections between them. These two forms of multiplicity are directly analogous to configurational and conformational entropy that drive clustering and arrangement in other systems [38]. A well-studied example of this is the self-assembly of tethered nanoparticles.[39] In these nanoscale systems, a subtle interplay between the entropy of the nanoparticle configurations and the conformations of polymer tethers drives complex, emergent organization, including the clustering of non-attracting objects.[40] The existence of a nanoscale analogue of the behaviour we observed in our naval architecture model strongly suggests the model behaviours we observed signal a manifestation of a more general phenomenon.

To see this, consider a generalization of the model arrangement problem we analyzed above. The general model is a system of N elements to be placed at some positions $\vec{x}_i$ in a domain D, where the subscript labels the element, and the vector components are coordinates of the position of that element. It is most concrete to think of the coordinates describing positions in physical space, however they could also describe positions in the space of element specifications (e.g., power consumption). We consider a situation in which some of the objects are functionally connected to one another, and some are not, which we encode in an adjacency matrix A_{ij}, which is one if elements i and j are functionally connected and zero if they are not.

Understanding whether clustering occurs in arranging design elements requires a means to generate arrangements systematically. Systematically generating candidate solutions to a problem that makes minimal assumptions about the form of the solutions is governed the theory of information.[41] Information theory shows [32] that generating solutions scored by a design objective, here the length of the routes between elements $L(\vec{x}_i, \vec{x}_j)$, is described by the generating function

$$Z(\beta) = \sum_{\{\vec{x}_i \in D\}} \sum_{\{R(\vec{x}_i, \vec{x}_j)\}} e^{-\beta \sum_{i,j} A_{ij} L(\vec{x}_i, \vec{x}_j)} \tag{1}$$

where $\beta = 1/T$ is the inverse of the tolerance for non-minimal routing, and $R(\vec{x}_i, \vec{x}_j)$ is the set of possible connection routes between $\vec{x}_i$ and $\vec{x}_j$. $Z(\beta)$, which is known as a partition function in statistical mechanics, is a Laplace transform of the design objective that generates candidate arrangements at a frequency weighted by a pressure β for minimal routing. I.e., at large β (equivalent to $T \to 0$), Equation (1) generates only arrangements with minimal or near-minimal routes, and generates routes of increasing L as $\beta \to 0$ (equivalent to $T \to \infty$).

The form of arrangements that Z generates is determined by how the multiplicity of options for routing a connection grows with the connection length. To see this, take the cardinality of the set of routes R between $\vec{x}_i$ and $\vec{x}_j$ as $\Omega(R(\vec{x}_i, \vec{x}_j))$ which gives the

generating function as

$$Z(\beta) = \sum_{\{\vec{x}_i \in D\}} e^{-\beta \sum_{i,j} A_{ij} \left(L(\vec{x}_i, \vec{x}_j) - \frac{1}{\beta} \ln \Omega(R(\vec{x}_i, \vec{x}_j)) \right)} \tag{2}$$

The factor in the exponent can be written as an effective distance

$$\Delta(\vec{x}_i, \vec{x}_j) = L(\vec{x}_i, \vec{x}_j) - T \ln \Omega(R(\vec{x}_i, \vec{x}_j)) \tag{3}$$

which expresses that routing multiplicity Ω counteracts the drive for minimal length L with a strength that is determined by the threshold for non-minimal routing T. Notably, $\ln \Omega$ is the Boltzmann entropy in statistical mechanics, the same physical property that drives clustering observed at the nanoscale.[39, 40] This quantitatively connects known nanoscale clustering mechanisms to arrangement clustering. In routing problems where $\ln \Omega(R(\vec{x}_i, \vec{x}_j))$ grows sufficiently fast, e.g. combinatorially, there will be a threshold T that induces $\Delta(\vec{x}_i, \vec{x}_j) < 0$ via entropic repulsion.

In microscopic systems, entropic repulsion generates clustering at inhomogeneities either generated by symmetry breaking [39, 40] or at pre-existing inhomogeneities at boundaries. [42] Bounded, inhomogeneous domains, which induce sites of microscale clustering,[42] are also generic in distributed systems. In our model system, it was precisely at boundary inhomogeneities clustering emerged, and this phenomenon should be generic.

Our analysis indicates that clustering occurs generically, and is driven by one of two mechanisms. Design elements can cluster to minimize connection distance, i.e. by minimizing $|\Delta|$ for $\Delta > 0$ in Equation (3). Or, elements can cluster emergently by entropic repulsion, i.e. by maximizing $|\Delta|$ for $\Delta < 0$ in Equation (3). Since cluster occurs for both $\Delta > 0$ and $\Delta < 0$, the only way to avoid clustering is if $\Delta \approx 0$ for separation distances that are larger than the characteristic R_g of attraction-driven clusters and smaller than the separation distance of boundary inhomogeneities where repulsion-driven clusters localize. However, when $\Delta \approx 0$, the effects of minimal routing length and routing multiplicity counteract one another. In this regime, the system is driven by the configurational entropy of the arrangement of the elements, with the result being large variability in L. This means that avoiding clustering only occurs at the expense of high variability in the design objective.

3. Discussion

Technical systems that manifest the adage that there is "no free lunch" have been identified in studies of search and optimization algorithms, where a series of theorems about algorithm performance averaged over all problem instances [43, 44]. It was shown it is impossible to select an *a priori* better algorithm unless one knows particular features of search or optimization landscapes that can be exploited, such as smoothness, differentiability, or convexity. Many similar no free lunch results have been proven for other problem domains [45], including community detection on networks where no

algorithm is optimal for finding communities across all types of networks [46]. Real-world networks are, however, very rarely unstructured, and any realistic structure can be exploited to improve the algorithm, leading to a "cheap lunch" effect [47].

While search and optimization results rely on a single optimality criterion to deny the free lunch, our results suggest the appearance of distinct mechanisms of non-optimality. Though we set out to solve a distributed system arrangement problem in such a way as to disrupt clustering, we discovered that disrupting clustering can only be achieved at the cost of design uncertainty. If we had *a priori* valuation of clustering avoidance over design uncertainty (or vice versa), we would readily prefer a particular T regime over others. This behaviour is, however, precisely the exploitation of prior knowledge that allows one to circumvent the no free lunch theorems in other domains. While our system shows two distinct failure modes of the design process, clustering and uncertainty, it is useful to draw connections to the clustering effects that appear in other contexts.

The clustering effects we observed in this paper depends on the close interplay of network topology and spatial constraints [48], but is distinct from the effects reported in many spatial network studies. Space-first studies usually first fix the spatial locations of the nodes and either study the empirical topology of the links, or propose a distance-based model of link probability [49]. Depending on the model parameters, the resulting spatial networks can manifest different global topological features, such as the small-world effect, topological clustering, or assortative mixing by node degree [50, 51]. In contrast, network-first studies start with a network topology and map nodes to coordinates into a high-dimensional Euclidean or hyperbolic space to study community structure, link prediction, and network navigability [52, 53]. While those approaches illuminate many spatio-topological features of large real-world networks, neither is able to describe embedding a fixed network into a prescribed low-dimensional space with a fixed complex boundary.

Directly embedding networks into a low-dimensional space (2D or 3D) is important for two reasons: to provide manufacturing prescriptions as in our problem, or to visualize networks on paper or screens. When both nodes and edges have finite size and can't overlap, the resulting spatial embeddings show different regimes of complex structure and mechanical response, mirroring the constraints on neuronal connections in mammalian brains induced by the space [54]. When the space constrains our visualizations of networks to a 2D screen or page, the ambiguity of resulting pictures aids in exploratory data analysis [55]. The visual structure of such network layouts is often created through force-directed layout algorithms and thus naturally highlights the community structure of the network [53]. The network used in the present paper has a strongly disassortative and bipartite structure as connections only exist between low-degree and high-degree nodes, thus leading to the segregation of nodes by degree in the high T regime (Figure 2).

In this paper we explored the problem of embedding fixed networks into a low-dimensional space with a fixed boundary that has received little theoretical attention

despite its practical importance for systems from microprocessors to airlines [56, 57], where close spatial proximity of nodes leads to vulnerability. We show how the combinatorial space of possible routings necessarily gives rise to either attractive or repulsive clustering, or high design variability. With no *a priori* preference between those regimes, there is no problem-solving advantage at any value of T, and thus no free lunch. While the *existence* of spatial clusters is a necessity in low-T and high-T regimes, the *structure* of those clusters can be affected by the topological features of networks, such as broader degree distributions and assortative mixing. The clustering behaviour can also be different in systems with a much smaller number of routings $\ln \Omega(L) \lesssim L$, or systems that allow for more expensive, non-minimal routing paths.

We have shown that there is a complex mechanism involving the competing degrees of freedom and how element connectivity is arranged, and this competition of degrees of freedom drives emergent clustering. Furthermore, we have shown that the behaviour of clustering is dependent on the degree of connectivity of the design elements. This complex mechanism can be avoided altogether by adopting high variability configurations. Using the high variability strategy, while we lose the certainties in arrangement, the clustering vulnerabilities can be mitigated. Nevertheless, strategies that satisfy only one type of degrees of freedom by either adopting solutions at low T or high T also lead to emergent clustering, and hence creates clustering vulnerabilities. These trade offs in degrees of freedom shown in Figure 5 further emphasize that there is no free lunch in avoiding emergent clustering. If $\ln \Omega(L) \lesssim L$, then it is conceivable to buy out. This could open up strategies in situations where there are routing constraints.
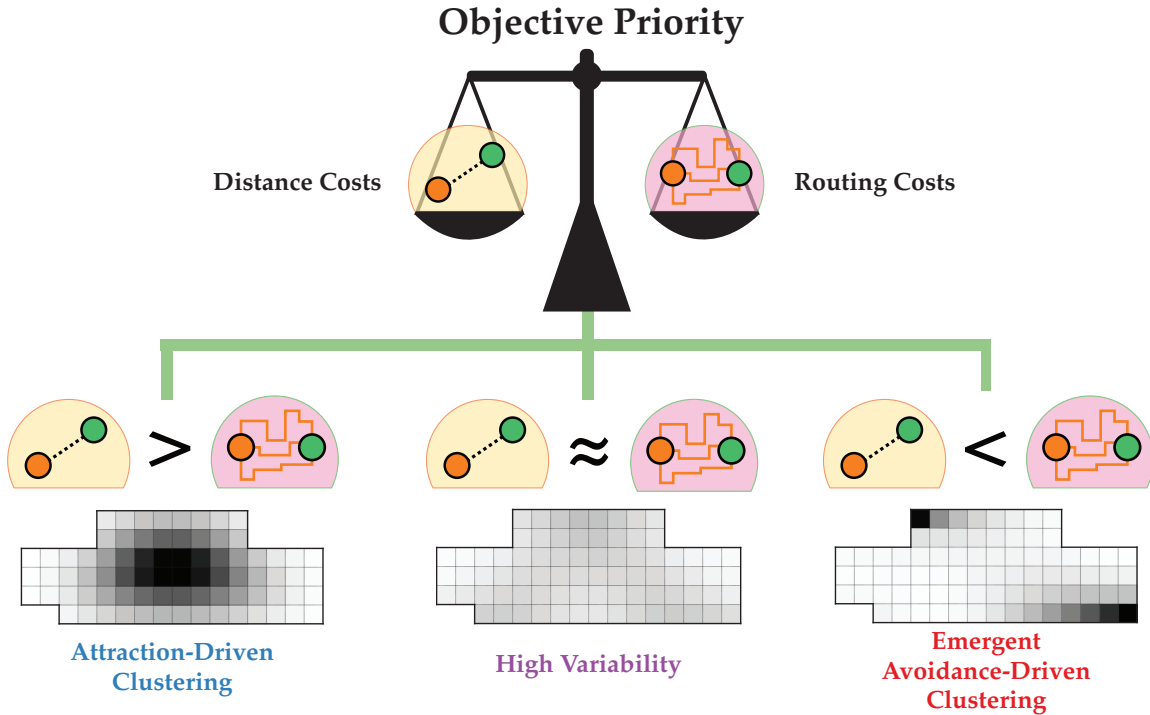
Figure 5.   **Trade-offs between multiple forms of clustering and objective variability imply there is no free lunch to disrupt clustering.** The attraction-driven clustering is an effect of the distance cost degrees of freedom, while the emergent avoidance-driven clustering is of the domination of the routing cost degrees of freedom. The configurations where the competing degrees of freedom are balanced produce high variability. Adopting high variability solutions circumvents the emergent clustering altogether.

4. Methods

4.1. Model

For the naval architecture model system, we chose the power system elements and connectivity from Ref. [13] shown in Panels I and II in Figure 1. The power sources, MAIN and AUX, are the design elements with high connectivity. The low-connectivity elements are not logically connected to one another. The chosen network is a practical arrangement of possible connectivity configurations. With this connectivity, we construct a thermodynamic model using Systems Physics [32].

For the design geometry of the model, we reproduce the geometry from Ref. [13] with twice the resolution in each axis, resulting in more available spaces for design elements to occupied. The geometry is chosen such that it reflects a practical requirement in naval ship design from Ref. [13]

To investigate the nature of clustering vulnerabilities, we created a computational method described in the following section to compute a vital statistical property known as partition function for the model distributed system. The model Naval Engineering

system contains 16 design elements of which 14 elements are low connectivity (degree $k \leq 2$) and 2 elements are high connectivity ($k > 2$). The logical connections between the elements are shown in panel (A) in Figure 3. To obtain a design solution/configuration, the elements are placed in the ship geometry. An example of a design solution for the model distributed system is shown in panel (II) in Figure 1.

4.2. Route Prioritization & Temperature

The two types of degrees of freedom, placement and routing, are encoded into the system via the objective function:

$$\Delta(\vec{x}_i, \vec{x}_j; T) = CL(\vec{x}_i, \vec{x}_j) - \frac{1}{T} \ln \Omega(R(\vec{x}_i, \vec{x}_j)) \tag{4}$$

where C is the cost scaling constant set to one in this study, L is the Manhattan distance between two points, and $\Omega(R(\vec{x}_i, \vec{x}_j))$ is the function which encodes the number of shortest path between two spatial positions. $\vec{x}_i$ denotes the position of the design element in the design geometry. On one hand, the placement degree of freedom is shown as Manhattan distance which requires more resources as the distance between any two elements increases. On the other hand, the routing is a competing degree of freedom where the number of shortest routings increases with the distance, acting against the placement degree of freedom. To examine the trade offs between the two degrees of freedom, we parametrize the priority for short, inexpensive connections through T dampening the Manhattan distance term. This T is mathematically equivalent to temperature.

Using the objective function from Equation (4), we calculate the partition function using methods from systems physics [48] shown as:

$$Z = \sum_{\alpha} e^{-\frac{1}{T} \sum_{i,j} A_{ij} \Delta(\alpha)} \tag{5}$$

where α denotes a *design solution* in a combinatorically large set of candidate designs α. A design solution α contains a configuration of the placements of the design elements in the model system. A_{ij} is the adjacency matrix of element connectivity represented by the network diagram in Panel I in Figure 1. We compute the partition function, using the computational package *Lachesis* [58], from design requirements using the tensor network construction demonstrated in Ref. [48].

With the requirements of the model system, we investigate the thermodynamic behaviour of each type of connectivity: high and low. The design elements that are logically connected should directly affect clustering since the objective function relies on the possible routing path and distance. We allow the system to vary the cost tolerance, T, where the resources are controlled such that we can examine clustering at various conditions. At low T, the design elements are penalized by being at a distance to one another, since the allowed resources are lower. While at high T, although the resources are more available, the cost of routing can be a key factor in penalizing certain expensive configurations. Thus, the clustering vulnerabilities may emerge from temperature conditions at both high and low T.

4.3. Critical Temperature Determination

In a system with the thermodynamic limit, one common indicator of a phase transition is the divergence of the isochoric heat capacity [36]. A phase transition indicates different regimes of thermodynamic behaviour, and hence, we utilize the temperature at which a phase transition occurs to define the boundary between two distinct regimes of behaviour. However, in a finite-sized system, the divergence manifests in the form of a maximum [59]. To determine the critical temperature T_c in our system, we identify the temperature at which the heat capacity is maximum as shown in Figure 3C.

4.4. Connectivity-Based Clustering: Radius of Gyration

For the effects of clustering from connections from any pair of elements, we use the order parameter radius of gyration. The radius of gyration quantifies the likelihood of a pair of chosen elements to be close to one another, and is defined by:

$$R_g = \left[\langle p(\vec{x}_i, \vec{x}_j)((\Delta_{ij}x)^2 + (\Delta_{ij}y)^2) \rangle \right]^{1/2} \tag{6}$$

where $p(\vec{x}_i, \vec{x}_j)$ denotes the two-point correlation function between two units i and j, and the difference Δ is calculated as the distance between two points. We use an average, denoted by $\langle \cdots \rangle$, of correlation and distance between all possible pairs of elements to determine the radius of gyration. Hence, the radius of gyration represents an average clustering between all pairs of elements.

Connectivity-Agnostic Clustering: Design Freedom. Measuring clustering without reference to element connectivity is akin to measuring how elements localize in a space. Emergent localization is a well-studied phenomenon in physics [60], and we follow Ref. [48] and use a normalized version of the existence area defined by

$$\Phi = \frac{1}{Y_0} \frac{\left(\sum_{\vec{x}} p(\vec{x}) \right)^2}{\sum_{\vec{x}} p(\vec{x})^2} \tag{7}$$

where the normalization Y_0 represents the number of available cells in the system, and $p(\vec{x})$ is a distribution of unit arrangements. In this form, Φ is bounded above by one when $p(\vec{x})$ is uniform, and decreases monotonically to $1/Y_0$ as p becomes more localized. Because Φ describes the effective fraction of the total area free to unit placement, we refer to this as design freedom.

4.5. Design Objective Uncertainty

For the heat capacity, we find that it has a maximum at a temperature at which we define as a critical temperature of the model system. A divergence in heat capacity is an indicator of a phase transition in magnetic or other conventional thermodynamic systems [36]. The present system is finite-sized, so the heat capacity cannot diverge. A maximum in heat capacity indicates that there are distinct regimes of behaviour. In

our case, the maximum in heat capacity suggests that there may be different behaviour in the temperature regimes separated by the maximum. Consequently, we define the temperature T_c at which the maximum occurs as the critical temperature in the system. Panel C in Figure 3 shows a finite maximum of heat capacity of the model system which we use to define the critical temperature.

Acknowledgements

References

[1] Shields C P and Singer D J 2017 *Naval Engineers Journal* **129** 75–86

[2] Kuhnle A, Nguyen N P, Dinh T N and Thai M T 2017 *Social Network Analysis and Mining* **7** 8 ISSN 1869-5450, 1869-5469

[3] Holme P and Kim B J 2002 *Physical Review E* **65** 026107 ISSN 1063-651X, 1095-3787

[4] Nesti T, Zocca A and Zwart B 2018 *Physical Review Letters* **120** 258301

[5] Dueñas-Osorio L and Vemuru S M 2009 *Structural Safety* **31** 157–167 ISSN 0167-4730

[6] Albert R, Jeong H and Barabási A L 2000 *Nature* **406** 378–382 ISSN 0028-0836, 1476-4687

[7] Albert R and Barabási A L 2002 *Reviews of Modern Physics* **74** 47–97 ISSN 0034-6861, 1539-0756

[8] Sun S, Liu Z, Chen Z and Yuan Z 2007 *Physica A: Statistical Mechanics and its Applications* **373** 851–860 ISSN 03784371

[9] Hu J S, Nadgir A, Vijaykrishnan N, Irwin M J and Kandemir M 2003 Exploiting program hotspots and code sequentiality for instruction cache leakage management *Proceedings of the 2003 International Symposium on Low Power Electronics and Design - ISLPED '03* (Seoul, Korea: ACM Press) p 402 ISBN 978-1-58113-682-1

[10] Yang C L and Lee C H 2004 HotSpot cache: Joint temporal and spatial locality exploitation for i-cache energy reduction *Proceedings of the 2004 International Symposium on Low Power Electronics and Design - ISLPED '04* (Newport Beach, California, USA: ACM Press) p 114 ISBN 978-1-58113-929-7

[11] Ceria A, Köstler K, Gobardhan R and Wang H 2021 *PLOS ONE* **16** e0245043 ISSN 1932-6203

[12] Fageda X and Flores-Fillol R 2016 *Regional Science and Urban Economics* **56** 73–81 ISSN 01660462

[13] Shields C P, Rigterink D T and Singer D J 2017 *Ocean Engineering* **135** 236–245 ISSN 0029-8018

[14] Keane R G, Deschamps L and Maguire S 2014 Reducing Detail Design and Construction Work Content by Cost-Effective Decisions in Early Stage Naval Ship Design *Day 2 Thu, October 23, 2014* (Houston, Texas, USA: SNAME) p D021S004R004

[15] Sharma C S, Tiwari M K, Zimmermann S, Brunschwiler T, Schlottig G, Michel B and Poulikakos D 2015 *Applied Energy* **138** 414–422 ISSN 03062619

[16] Sharma C S, Tiwari M K and Poulikakos D 2016 *Applied Thermal Engineering* **93** 1314–1323 ISSN 13594311

[17] Tschanz J, Yibin Ye, Liqiong Wei, Govindarajulu V, Borkar N, Burns S, Karnik T, Borkar S and De V 2002 Design optimizations of a high performance microprocessor using combinations of dual-V/sub T/ allocation and transistor sizing *2002 Symposium on VLSI Circuits. Digest of Technical Papers (Cat. No.02CH37302)* (Honolulu, HI, USA: IEEE) pp 218–219 ISBN 978-0-7803-7310-5

[18] Doerry N 2007 *ASNE Naval Engineers Journal* **119** 25–34

[19] Goodrum C J, Shields C P and Singer D J 2018 *Ocean Engineering* **150** 36–47 ISSN 00298018

[20] Habben Jansen A, Kana A and Hopman J 2019 *Ocean Engineering* **190** 106448 ISSN 00298018

[21] Habben Jansen A 2020 *A Markov-based Vulnerability Assessment of Distributed Ship Systems in the Early Design Stage* Ph.D. thesis Delft University of Technology

[22] Watts D J and Strogatz S H 1998 *Nature* **393** 440–442 ISSN 0028-0836, 1476-4687

[23] Holme P, Kim B J, Yoon C N and Han S K 2002 *Physical Review E* **65** 056109 ISSN 1063-651X, 1095-3787

[24] Whitcomb C A 1998 *Naval Engineers Journal* **110** 49–63 ISSN 00281425, 15593584

[25] Watson D G M 1998 *Practical Ship Design* 1st ed (*Elsevier Ocean Engineering Book Series* no v. 1) (Amsterdam ; New York: Elsevier) ISBN 978-0-08-042999-1

[26] Cui S, Madan R, Goldsmith A and Lall S 2007 *IEEE Transactions on Wireless Communications* **6** 3688–3699 ISSN 1536-1276

[27] Benini L and De Micheli G Jan/2002 *Computer* **35** 70–78 ISSN 00189162

[28] Jiang X, Shokri-Ghadikolaei H, Fodor G, Modiano E, Pang Z, Zorzi M and Fischione C 2019 *Proceedings of the IEEE* **107** 280–306 ISSN 0018-9219, 1558-2256

[29] Benford H 1967 *Marine Technology and SNAME News* **4** 519–536 ISSN 0025-3316, 1542-0566

[30] Habben Jansen A C, Duchateau E A E, Kana A A and Hopman J J 2020 *Journal of Marine Engineering & Technology* **19** 45–61 ISSN 2046-4177, 2056-8487

[31] Brownlow L C, Goodrum C J, Sypniewski M J, Coller J A and Singer D J 2021 *Ocean Engineering* **225** 108731 ISSN 00298018

[32] Klishin A A, Shields C P, Singer D J and van Anders G 2018 *New Journal of Physics* **20** 103038 (*Preprint* `1709.03388`)

[33] Kamide K and Dobashi T 2000 *Physical Chemistry of Polymer Solutions: Theoretical Background* 1st ed (Amsterdam ; New York: Elsevier Science BV) ISBN 978-0-444-89430-4

[34] de Gennes P G 1979 *Scaling Concepts in Polymer Physics* (Cornell University Press) ISBN 978-0-8014-1203-5

[35] Filoche M and Mayboroda S 2009 *Physical Review Letters* **103** 254301

[36] Goldenfeld N 1992 *Lectures on Phase Transitions and the Renormalization Group* (Reading MA: Addison-Wesley)

[37] Sethna J 2021 *Statistical Mechanics: Entropy, Order Parameters, and Complexity* (Oxford University Press, USA)

[38] King E M, Gebbie M A and Melosh N A 2019 *Langmuir : the ACS journal of surfaces and colloids* **35** 16062–16069

[39] Zhang, Zhenli, Horsch M A, Lamm M H and Glotzer S C 2003 *Nano Letters* **3** 1341–1346

[40] Marson R L, Nguyen T D and Glotzer S C 2015 *MRS Communications* **5** 397–406

[41] Shannon C 1948 *Bell System Technical Journal* **27** 379–423, 623–656

[42] Dinsmore AD, Yodh AG and Pine DJ 1996 *Nature* **383** 239–242

[43] Wolpert D H and Macready W G 1995 No free lunch theorems for search Working papers Santa Fe Institute

[44] Wolpert D and Macready W 1997 *IEEE Transactions on Evolutionary Computation* **1** 67–82 ISSN 1089778X

[45] Adam S P, Alexandropoulos S A N, Pardalos P M and Vrahatis M N 2019 No Free Lunch Theorem: A Review *Approximation and Optimization* vol 145 ed Demetriou I C and Pardalos P M (Cham: Springer International Publishing) pp 57–82 ISBN 978-3-030-12766-4 978-3-030-12767-1

[46] Peel L, Larremore D B and Clauset A 2017 *Science Advances* **3** e1602548 ISSN 2375-2548

[47] Peixoto T P and Kirkley A 2022

[48] Klishin A A, Singer D J and van Anders G 2021 *Journal of Physics: Complexity* **2** 025015 (*Preprint* `2010.00141`)

[49] Barthélemy M 2011 *Physics Reports* **499** 1–101 ISSN 03701573

[50] Makarov V V, Kirsanov D V, Frolov N S, Maksimenko V A, Li X, Wang Z, Hramov A E and Boccaletti S 2018 *Scientific Reports* **8** 13825 ISSN 2045-2322

[51] Boguñá M, Krioukov D, Almagro P and Serrano M Á 2020 *Physical Review Research* **2** 023040 ISSN 2643-1564

[52] Krioukov D, Papadopoulos F, Kitsak M, Vahdat A and Boguñá M 2010 *Physical Review E* **82** 036106 ISSN 1539-3755, 1550-2376

[53] Zhang Y J, Yang K C and Radicchi F 2021 *Physical Review E* **104** 044315 ISSN 2470-0045, 2470-0053

[54] Dehmamy N, Milanlouei S and Barabási A L 2018 *Nature* **563** 676–680 ISSN 0028-0836, 1476-4687

[55] Venturini T, Jacomy M and Jensen P 2021 *Big Data & Society* **8** 205395172110184 ISSN 2053-9517, 2053-9517

[56] Hamann H F, Weger A, Lacey J A, Hu Z, Bose P, Cohen E and Wakil J 2007 *IEEE Journal of Solid-State Circuits* **42** 56–65 ISSN 0018-9200

[57] Lavandier J, Islami A, Delahaye D, Chaimatanan S and Abecassis A 2021 *Aerospace* **8** 288 ISSN 2226-4310

[58] Chitnelawong P, Klishin A A, MacKay N and van Anders G 2023 Lachesis Zenodo

[59] Chomaz Ph and Gulminelli F 1999 *Nuclear Physics A* **647** 153–171 ISSN 03759474

[60] Thouless D J 1974 *Physics Reports* **13** 93–142